NIH-PA Author Manuscript

Dominant connexin26 mutants associated with human hearing loss have trans-dominant effects on connexin30

Sabrina W. Yum[1,2], **Junxian Zhang**[2], and **Steven S. Scherer**[2]

[1] Division of Neurology, The Children's Hospital of Philadelphia

[2] Department of Neurology, University of Pennsylvania, Philadelphia, PA 19104

Abstract

Dominant mutations in *GJB2,* the gene encoding the human gap junction protein connexin26 (Cx26), cause hearing loss. We investigated whether dominant Cx26 mutants interact directly with Cx30. HeLa cells stably expressing nine dominant Cx26 mutants, six associated with non-syndromic hearing loss (W44C, W44S, R143Q, D179N, R184Q and C202F) and three associated with hearing loss and palmoplantar keratoderma (G59A, R75Q and R75W), individually or together with Cx30, were analyzed by immunocytochemistry, co-immunoprecipitation, and functional assays (scrape-loading and/or fluorescence recovery after photobleaching). When expressed alone, all mutants formed gap junction plaques, but with impaired intercellular dye transfer. When expressed with Cx30, all mutants co-localized and co-immunoprecipitated with Cx30, indicating they likely co-assembled into heteromers. Furthermore, 8/9 Cx26 mutants inhibited the transfer of neurobiotin or calcein, indicating that these Cx26 mutants have trans-dominant effects on Cx30, an effect that may contribute to the pathogenesis of hearing loss.

Keywords

gap junctions; immunoprecipitation; dye transfer; FRAP; Cx26; Cx30

INTRODUCTION

Gap junctions allow the direct passage of ions and small molecules (typically < 1000 Da) between adjacent cells, and are thought to have diverse functions, including the propagation of electrical signals, metabolic cooperation, spatial buffering of ions, growth control, and cellular differentiation (Bruzzone et al., 1996; Harris, 2001). They are formed by two apposed hemichannels (or connexons); a complete channel is formed when one hemichannel docks with a compatible hemichannel on an apposed cell membrane. Each hemichannel is comprised of six compatible connexin molecules - a large family of highly conserved proteins, named according to their predicted molecular mass (Willecke et al., 2002). Individual hemichannels can be composed of one (homomeric) or more than one (heteromeric) type of connexin. Similarly, channels can be composed of hemichannels comprised of the same (homotypic) or different (heterotypic) connexins (Kumar and Gilula, 1996; White and Bruzzone, 1996). Any

Address for correspondence: Sabrina W. Yum, M.D., Division of Neurology, Children's Hospital of Philadelphia, Abramson Research Center, Room 502A, 34th Street and Civic Center Boulevard, Philadelphia, PA 19104, Phone: 215-590-1710, FAX: 215-590-1771, yums@email.chop.edu.

two compatible connexins can theoretically form 196 different channels (Brink et al., 1997) whose biophysical properties (such as permeability and gating) may be different from their homomeric homotypic counterparts(Brink et al., 1997).

Mutations in *GJB2*, *GJB6,* and *GJB3*, the genes that encode the human gap junction proteins connexin26 (Cx26), Cx30, and Cx31, respectively, cause hearing loss (Estivill et al., 1998; Grifa et al., 1999; Kelsell et al., 1997; Xia et al., 1998). *GJB2* mutations are the most common cause of hereditary non-syndromic hearing loss (NSHL), with over 90 recessive mutations reported (http://davinci.crg.es/deafness/). Dominant mutations in *GJB2* also cause hearing loss, either in isolation (non-syndromic) or as part of a syndrome associated with various skin disorders. Recessive *GJB2* mutations likely cause simple loss of function, whereas dominant *GJB2* mutations likely cause gain of function, including dominant-negative effects on wild type Cx26 and/or Cx30 (Marziano et al., 2003) because haplotype insufficiency of *GJB2* does not cause hearing loss based on the observation that the heterozygous parents of deaf children (who have homozygous *GJB2* mutations) do not themselves have hearing loss.

Cx26 and Cx30 are the major gap junction proteins expressed in cochlea with broadly overlapping but not identical distributions (Ahmad et al., 2003; Forge et al., 2002; Jagger and Forge, 2006; Kikuchi et al., 1995; Lautermann et al., 1998; Liu and Zhao, 2008; Sun et al., 2005; Zhao and Yu, 2006). They have been co-immunoprecipitated from mouse cochlear homogenates and transfected cells co-expressing them (Ahmad et al., 2003; Di et al., 2005; Forge et al., 2003; Sun et al., 2005; Yum et al., 2007), indicating that they form hybrid heteromeric/heterotypic gap junction channels. Here, we investigated whether similar interactions occur between Cx30 and nine dominant Cx26 mutants (Fig. S1) - six (W44C, W44S, R143Q, D179N, R184Q and C202F) that cause NSHL and three (G59A, R75Q and R75W) that cause syndromic hearing loss (SHL) associated with palmoplantar keratoderma (PPK). All mutants co-localized and co-immunoprecipitated with Cx30, and 8/9 had different degrees of trans-dominant effects on the function of Cx30; providing further evidence that these dominant effects contribute to the pathogenesis of hearing loss.

RESULTS

All 9 dominant Cx26 mutants form gap junction-like plaques

To investigate the biology of *GJB2* mutations, we expressed wild type *GJB2* and 9 different dominant *GJB2* mutations (Fig. S1) by transfection into communication-incompetent HeLa cells, followed by bulk-selection. Immunostaining with a rabbit antiserum against the C-terminus of Cx26 demonstrated gap junction plaques (GJPs) on apposing cell membranes for cells expressing wild type Cx26 and all 9 (W44C, W44S, G59A, R75Q, R75W, R143Q, D179N, R184Q, C202F) mutants (Fig. 1). A monoclonal antibody against the C-terminus of Cx26 and a rabbit antiserum against the intracellular loop gave similar results (data not shown). Cells transfected with the vector alone or parental HeLa cells were not labeled with any of these antibodies (data not shown). Except for cells lines expressing two individual mutants (G59A and D179N) that had low expression of Cx26, between 60% to nearly 100% of the bulk-selected cells expressed Cx26, depending on the mutation and the cell line. Immunoblot analysis of these cell lines with the rabbit antiserum against the C-terminus demonstrated a band (26 kDa) that was absent both in parental HeLa cells and in cells expressing the vector (pIRESpuro3) alone (Fig. S2 and data not shown). Thus, most dominant Cx26 mutants linked to NSHL and some mutants linked to SHL associated with PPK form GJPs that appear similar to those formed by wild type Cx26.

Dominant Cx26 mutants have impaired function

To investigate whether the gap junction channels formed by these dominant Cx26 mutants are functional, we performed scrape-loading assays (El-Fouly et al., 1987) on bulk-selected cell lines with expression in at least 60% of the cells. In this assay, confluent plates of cells are wounded with a scalpel blade in the presence of Lucifer Yellow (LY; 457 Da, −2 charge) or neurobiotin (NB; 323 Da; +1), a non-fluorescent tracer that can be visualized with fluorescently-conjugated avidin after fixation (Elfgang et al., 1995). Neither tracer diffused beyond the wounded parental cells (data not shown), confirming that they are communication-incompetent (Yum et al., 2007). Cells stably expressing wild type Cx26 robustly transferred both LY and NB, whereas none of the cells expressing these seven Cx26 mutants (W44C, W44S, R75Q, R75W, R143Q, R184Q, and C202F) passed either tracer (Fig. 2). We performed the scrape-loading assay on at least 2 different cell lines for each mutation and the experiments were repeated at least 3 times, with similar results.

We were unable to generate high expression bulk-selected cell lines for G59A and D179N, so we adapted our protocol (Yum et al., 2007) for fluorescence recovery after photobleaching (FRAP) to transiently transfected cells, using a bicistronic vector (pIRES2-DsRed). About 40 hours after transfection, confluent monolayers of cells were incubated in calcein AM, which is cleaved within cells, yielding calcein, a small (623 Da; −4 charge) fluorescent molecule. Individual DsRed-positive cells that were in close contact with at least three other DsRed-positive cells were photobleached, and images were acquired immediately before and after bleaching, and every 10 seconds thereafter for 400 seconds. The fluorescence was measured as mean pixel density in the bleached cell in every image. We normalized the data for each cell, assigning the fluorescent signal present immediately prior and immediately after photobleaching as 100% and 0%, respectively, so that the data from different cells could be pooled. The results are shown in Figure 3, which depicts the mean percent recovery plotted against time post-bleaching. Cells expressing wild type Cx26 recovered 51% of their pre-bleach signal 400 sec after bleaching, whereas cells expressing G59A or the vector alone showed no recovery. Cells expressing D179N recovered partially after bleaching, but the rate and the amount was significantly less than for cells expressing wild type Cx26 ($p < 0.0001$) at all time points. Thus, in contrast to G59A and the other mutants, D179N formed partially functional channels.

Dominant Cx26 mutants form gap junction plaques with Cx30

To determine whether dominant Cx26 mutants could interact with Cx30, we transfected HeLa cells that stably expressed Cx30 (with a puromycin-resistance vector, Yum et al., 2007) with a G418 resistance vector containing *GJB2* mutations, thereby obtaining bulk-selected cells that expressed both Cx30 and individual Cx26 mutants. Because Cx26 and Cx30 are closely related (Willecke et al., 2002), and some antibodies against them cross-react (Nagy et al., 1997), we used antibodies that we previously found not to cross react - a rabbit antiserum against the C-terminus of Cx30 combined with the mouse monoclonal antibody against the C-terminus of Cx26 (Yum et al., 2007). As shown in Figure 4, bulk-selected cells expressing wild type Cx30 and Cx26 or individual Cx26 mutants had GJPs comprised of both connexins. We found similar results with at least 3 different cell lines for each mutant. Cells co-transfected with the expression plasmid and Cx30 or Cx26 were labeled with the Cx30 antibody or the Cx26 antibody only, respectively, and parental HeLa cells were not labeled with either antibody (data not shown).

Dominant Cx26 mutants co-immunoprecipitate with Cx30

Their co-localization suggests that the Cx26 mutants form heteromeric hemichannels with Cx30. Because Cx30 and Cx26 can be reciprocally co-immunoprecipitated from transfected cells, indicating that they form hybrid heteromeric/heterotypic channels (Di et al., 2005; Sun

et al., 2005; Yum et al., 2007), we investigated whether Cx30 and Cx26 mutants can interact the same way. Lysates from bulk-selected cells expressing Cx26 and/or Cx30 were immunoprecipitated with a mouse monoclonal antibody against the C-terminus of Cx26, and the immunoprecipitate was probed with a rabbit antiserum against the C-terminus of Cx30, using the two antibodies that do not cross-react (Yum et al., 2007). As shown in Figure 5, Cx30 was present in the immunoprecipitates from cells that co-expressed Cx30 and wild type Cx26 or one of the Cx26 mutants (panels a & c), indicating that they interact directly, but was not present in the immunoprecipitates from cells expressing Cx26 alone or Cx30 alone (panel a), confirming that the Cx26 and Cx30 antibodies not cross react with each other. Rehybridizing the blot with a rabbit antiserum against Cx26 demonstrated that Cx26 was present in the appropriate samples (panels b & d). This experiment was performed twice with similar results, and similar results were also obtained from transiently transfected cells (data not shown). To determine if the interaction demonstrated was heteromeric or heterotypic interaction or both, we also performed the same co-IP experiment using co-culture where Cx26 and Cx30 stable cells admixed at 1:1 ratio 2 days prior to the experiments. As shown in Figure 5e, Cx30 was also present in the immunoprecipitates from the Cx26+Cx30 co-culture cells, but the signal was much less intense then that from cells co-expressing Cx26/Cx30 (while the intensity of the bands for Cx26 was similar when the membrane was re-blotted with a rabbit antiserum against Cx26 as shown in Fig. 5f), indicating both heteromeric and heterotypic interaction was present in cells co-expressing Cx26/Cx30. As an additional control, we performed the same experiment using cells co-expressing Cx26 and Cx43, which do not interact directly in mammalian cells (Gemel et al., 2004). Cx43 did not co-immunoprecipitate with Cx26, but was found in the unbound fraction (Fig. 5g). Thus, Cx26 and Cx30 interact directly by forming hybride heteromeric/heterotypic channels, and this interaction is specific.

Functional analysis of Cx30 stable cells co-expressing Cx26 mutants

To investigate the functional properties of channels comprised of a Cx26 mutant and wild type Cx30, we performed scrape-loading on bulk-selected cells co-expressing Cx30 and individual Cx26 mutants. As shown in Figure 6A, we confirmed that cells stably co-expressing Cx30 and wild type Cx26 had less extensive LY transfer than did cells expressing wild type Cx26 alone, whereas cells stably expressing Cx30 alone did not transfer LY (Beltramello et al., 2003; Elfgang et al., 1995; Manthey et al., 2001; Marziano et al., 2003; Yum et al., 2007; Zhao, 2005). In contrast, cells co-expressing Cx30 and W44C, W44S, R75Q, R75W, R143Q, R184Q, or C202F did not transfer LY. Occasional LY transfer was also observed in cells co-expressing Cx30 and G59A, and cells co-expressing D179N showed extensive LY transfer, although less extensive as compared to cells co-expressing Cx30 and wild type Cx26. To exclude the possibility of dye passage from cell to cell through other mechanisms such as cytoplasmic bridges, we also scrape-loaded cells with 10,000 Da tetramethylrhodamine dextran, which does not permeate gap junctions; this was confined to the scrape-loaded cells (data not shown). For each mutation, the scrape-loading assay was repeated 2–4 times on at least 2 different cell lines, with similar results. Thus, as compared to Cx26, these dominant Cx26 mutants had impaired LY transfer when expressed alone or co-expressed with Cx30.

Because Cx30 homotypic channels are minimally permeable to LY, the lack of transfer of Lucifer yellow in cells co-expressing Cx30/Cx26 mutant could result from the loss of Cx26 function in the Cx30/Cx26 hybrid channels (and does not provide evidence of dominant negative effects). Therefore, we performed scrape-loading using (positively charged) NB, as a more direct test to determine whether these Cx26 mutants had dominant effects on Cx30. Dye transfer was quantified by measuring the distance from the scrape line to the point where the average fluorescence intensity dropped to 1.5x the background intensity, and the difference between cells co-expressing Cx30 and the expression vector and cells co-expressing Cx30 and individual mutants was compared using ANOVA (GraphPad Prism 4 software, San Diego,

CA). As shown in Figure 6B and quantified in Figure 6C, cells expressing Cx30 alone showed extensive transfer of NB to neighboring cells (Beltramello et al., 2003; Elfgang et al., 1995; Manthey et al., 2001; Marziano et al., 2003; Sun et al., 2005; Yum et al., 2007), and even more extensive transfer when this cell line was transfected to co-express wild type Cx26 (Yum et al., 2007). In contrast, three mutants (W44C, R75W, C202F) completely inhibited ($p < 0.0001$), four mutants (W44S, G59A, R75Q, R184Q) partially inhibited ($p < 0.0001$), and two mutants (R143Q, D179N) did not demonstrably inhibit NB transfer ($p > 0.05$) when compared to cells co-expressing Cx30 and the expression vector. To demonstrate that a lack of Cx26 expression did not confound these findings, we immunolabeled the scrape-loaded cells for Cx30 and Cx26, and only used regions with definite co-expression of both Cx30 and Cx26 for the analysis; examples are shown in Figure S3 in supplementary materials. These scrape-loading assays were repeated 2–4 times on at least 2 different cell lines for each mutation, with similar results.

As an independent test of whether cells co-expressing Cx30 and individual Cx26 mutants formed functional channels, we performed FRAP using calcein AM (see Methods), as calcein can pass readily through gap junctions comprised of Cx26 alone or both Cx26 and Cx30, but substantially less through those comprised of Cx30 alone (Yum et al., 2007). The fluorescence recovery curves of cells co-expressing Cx30 and individual mutants were compared to those of cells co-expressing Cx30 and the vector alone (vector/Cx30) or Cx30 and wild type Cx26 (Cx26/Cx30), using a repeated measures regression model for the transformed percentages (see Methods). As shown in Figure 7 and Table S1, cells co-expressing Cx30 and G59A were substantially less permeable to calcein as compared to cells co-expressing Cx26/Cx30 ($p < 0.0001$), but similar to cells co-expressing vector/Cx30 (Yum et al., 2007), whereas cells co-expressing Cx30 and seven of the individual Cx26 mutants (W44C, W44S, R75Q, R75W, R143Q, R184Q, C202F) showed significantly less recovery than did cells co-expressing vector/Cx30 ($p < 0.0001$). Cells co-expressing Cx30 and D179N showed more recovery than did cells co-expressing vector/Cx30 ($p < 0.0001$), but less recovery than cells co-expressing Cx26/Cx30 at all time points ($p < 0.0001$). Taken together, 8/9 mutants inhibited dye transfer when co-expressed with Cx30 using these two assays, indicating a dominant negative effect on Cx30.

DISCUSSION

Characterization of dominant Cx26 mutants

Up to 30 different dominant mutations in *GJB2* have been reported; 10 are associated with NSHL, and the others cause SHL with various skin diseases. The expression pattern in mammalian cells was investigated for 13 of these mutants (Common et al., 2003; de Zwart-Storm et al., 2008; Haack et al., 2006; Martin et al., 1999; Marziano et al., 2003; Matos et al., 2008; Oshima et al., 2003; Piazza et al., 2005; Richard et al., 2002; Stong et al., 2006; Thomas et al., 2004), but most of these studies primarily focused on mutations causing SHL, and majority of the mutants associated with the more severe forms of skin diseases were shown to have trafficking defects.

We investigated the expression pattern and dye transfer of 9 mutants associated with NSHL or SHL with the milder form of skin disease PKK; R143Q, D179N, R184Q, and C202F had not been investigated. Consistent with prior studies, W44C, W44S, R75Q, and R75W formed GJPs on apposing cell membranes when expressed alone (Martin et al., 1999; Marziano et al., 2003; Oshima et al., 2003; Piazza et al., 2005; Thomas et al., 2004). Our results also support the finding that a human G59A-GFP fusion protein formed GJPs (Thomas et al., 2004), but contradict a report that HeLa cells expressing G59A or G59A-GFP did not form GJPs (Marziano et al., 2003). Technical issues may account for their failure to detect GJPs - cells were transiently transfected by injection, and the mutation was made in the rat *Gjb2* gene.

We demonstrated (by scrape-loading and/or FRAP) that the homotypic channels composed of these 9 individual mutants had impaired permeability to LY, NB, and/or calcein. These results confirm and extend prior reports that cells expressing W44C, W44S, G59A, R75Q, or R75W failed to transfer similar tracers that were injected into single cells (Martin et al., 1999; Marziano et al., 2003; Oshima et al., 2003; Piazza et al., 2005; Thomas et al., 2004). Taken together, our data shows that many dominant Cx26 mutants that cause NSHL or SHL with PKK can form GJPs similar to that of wild type Cx26, but with severely impaired channel function, likely due to improper docking or defective gating.

Trans-dominant effects of Cx26 mutants on Cx30

All nine dominant Cx26 mutants were co-localized with Cx30, and 8/9 altered the permeability of cells expressing Cx30 to different degrees. D179N did not diminish the transfer of NB or calcein in cells expressing Cx30, whereas W44S, W44C, R75W, R75Q, R184Q, and C202F (but not R143Q) diminished the transfer of NB, and W44S, W44C, G59A, R75W, R75Q, R143Q, R184Q, and C202F (but not G59A) diminished the transfer of calcein. Our findings partially agree with prior report that W44S, G59A, and R75W incompletely inhibit NB transfer when co-injected with Cx30 (Marziano et al., 2003), and are consistent with the observation that R75W electrically uncoupled the channels formed by Cx26 and Cx30 in *Xenopus* oocytes (Chen et al., 2005). The variable trans-dominant effects perhaps owe to difference in the charge of NB (+1) versus calcein (−4) and the different structural changes caused by these mutants; most of the residues involved mediate intra- or inter-protomer interactions (Maeda et al., 2009). Although we cannot exclude the possible contribution of undetected differences in the level of expression, our data suggest that some Cx26 mutants (W44C, R75W, C202F) have stronger dominant effects on Cx30. It remains to be determined whether such differences contribute to the phenotypic manifestations in affected patients.

Interestingly, D179N did not completely abolish dye transfer, in contrast to previous report that this mutant near completely disrupt intercellular electrical coupling in transfected HEK293 cells (Zhang et al., 2005). Technical reason may have account for the discrepancy between its effect on ionic coupling and chemical coupling, as EGFP-tagged D179N was used for the electrophysiology study (Zhang et al., 2005) and epitope-tagged connexins may potentially affect the biophysical properties of the channels (Bukauskas et al., 2001; Sullivan and Lo, 1995). D179N occurs in a highly conserved residue in the extracellular loop that is shown to mediate inter-connexon interaction (Maeda et al., 2009), and was identified in a family with four affected members presenting mild-to-moderate post-lingual hearing loss (Primignani et al., 2003); whether the partially functional channels account for the milder phenotype in this family, and whether a dominant effect can be demonstrated with other functional assays remain to be determined.

The interactions between Cx30 and the other six mutants we studied (W44C, R75Q, R143Q, D179N, R184Q, and C202F) had not been previously analyzed. Altogether, the present study provides the most comprehensive data, including the first demonstration that dominant Cx26 mutants co-immunoprecipitate with Cx30, thus, confirming their direct interaction (likely by co-assembling into hybrid heteromeric/heterotypic channels), and further supporting the idea that Cx26 mutants have trans-dominant effects on Cx30.

How do dominant GJB2 mutations cause hearing loss?

Both dominant and recessive *GJB2* mutations cause hearing loss. Because people who are heterozygous for recessive *GJB2* mutations have no hearing impairment, haplotype insufficiency is not sufficient to cause hearing loss. Therefore, dominant mutants that result in hearing loss must have a gain of toxic function. Our results and those of others (Chen et al., 2005; Marziano et al., 2003) strongly support a dominant-negative mechanism of Cx26 mutants

on Cx30; whether these mutants also have comparable effects on wild type Cx26 remains to be determined, but seems likely given their high degree of homology. In this scenario, dominant Cx26 mutants affect hearing by diminishing the function of Cx26 and/or Cx30, although separating these two effects would require a full understanding of the roles of Cx26 and Cx30 in the cochlea. Other dominant effects are possible. Some Cx26 mutations associated with keratitis-ichthyosis-deafness syndrome cause cell death due to aberrant hemichannel activity (Gerido et al., 2007; Lee et al., 2009; Stong et al., 2006). However, this has not been demonstrated in dominant mutations associated with NSHL or SHL with milder forms of skin diseases, and some of these mutants have been shown to increase cell survival instead (Common et al., 2004).

The roles of Cx26 and Cx30 in cochlea have yet to be determined, although it is clear that both are required for hearing (Cohen-Salmon et al., 2002; Teubner et al., 2003). It has been proposed that GJs are involved in ionic coupling, allowing endolymphatic K^+ recycling and the generation of endocochlear potential after the onset of hearing (Wangemann, 2002), but this has yet to be directly demonstrated. Furthermore, this hypothesis would not explain the recent findings that normal postnatal maturation and development of the organ of Corti was affected in conditional *Gjb2*-null mice (Wang et al., 2009) and in a transgenic mouse model expressing a dominant negative R75W mutant (Inoshita et al., 2008) before the onset of hearing. Another idea is that GJs mediate metabolic coupling in the cochlea, allowing the exchange of larger molecules such as metabolites, second messengers and glucose (Beltramello et al., 2005; Chang et al., 2008; Zhang et al., 2005). In this scenario, the co-assembly of Cx26 and Cx30 increases the functional diversity of the gap junction network in cochlea as hybrid Cx26/Cx30 channels have properties distinct from those of homomeric homotypic channels comprised of Cx26 or Cx30 alone; they have faster intercellular Ca^{2+} signaling (Sun et al., 2005) and are more permeable to neurobiotin (Yum et al., 2007). Whether they have different permeability to metabolites and second messengers is not known, but there are precedents for this possibility (Harris, 2007).

Different mechanisms likely underlie hearing loss due to the absence of Cx26 or Cx30 as the pattern and time course of cellular degeneration in the cochlea of conditional *Gjb2*-null and *Gjb6*-null mice are very different (Sun et al., 2009). Although a question of whether Cx26 plays more important role than Cx30 in cochlear function has been raised (Ahmad et al., 2007), increasing evidence has shown that Cx30 plays an essential role for metabolic cooperation in the cochlea. In the absence of Cx30 (but the presence of homomeric Cx26 channels), the diffusion of various molecules (including a fluorescent glucose analogue 2-NBDG) is reduced and intracellular reactive oxygen species are increased among supporting cells of the cochlea, and the uptake of 2-NBDG from the blood circulation to cochlea is markedly reduced (Chang et al., 2008). Whether these effects are due to the loss of hybrid Cx26/Cx30 channels, or homomeric Cx30 channels, or both, remains to be determined. Nevertheless, these findings support the possibility that trans-dominant effect of Cx26 mutants on Cx30 affect the cellular energy supply and biochemical homeostasis in the cochlea, resulting in hearing loss. This argument is supported by the observation that *Gjb2*$^{+/−}$/*Gjb6*$^{+/−}$ double heterozygous mice have moderate hearing impairment (Michel et al., 2003), while neither *Gjb2*$^{+/−}$ or *Gjb6*$^{+/−}$ heterozygous mice exhibit hearing loss, indicating that the functional loss of one *GJB2* allele and one *GJB6* allele is sufficient to cause hearing impairment.

The mechanism underlying different types of skin diseases associated with dominant Cx26 mutations is likely to be complicated. Targeted epidermal expression of the D66H mutant causes reduction and cytoplasmic location of Cx30 in epidermis and mimics true Vohwinkel Syndrome, but whether this effect is the cause of the skin manifestation is less clear (Bakirtzis et al., 2003) because the *Gjb6*-null mice do not have a skin phenotype (Teubner et al., 2003). Although we did not directly investigate this issue, our data suggest that the trans-dominant

effect on Cx30 alone is less likely to account for the skin disease caused by mutations associated with PPK (G59A, R75W and R75Q), as no distinct differences in the pattern of change/ interactions with Cx30 (from that of NSHL mutations) have emerged. As in cochlea, gap junction communication plays a crucial role in keratinocyte growth and differentiation. Unlike in cochlea, however, Cx26 is not essential in the skin as patients with recessive *GJB2* mutations are deaf but do not have skin phenotypes. Besides Cx26 and Cx30, seven other connexins, including Cx30.3, Cx31, Cx31.1, Cx37, Cx40 and Cx43 have been reported to express in skin with distinct temporal and spatial expression patterns (Kelsell et al., 2001). Whether differential interaction of dominant Cx26 mutants and some of these connexins expressed in skin potentially explains the variable phenotypes needs to be systematically investigated.

MATERIALS AND METHODS

Mutant Cx26 expression constructs

A plasmid containing human *GJB2* (kindly provided by Dr. Bruce Nicholson) was amplified by PCR using oligonucleotide primers designed to include the open reading frame (ORF) and incorporate a 5' *NheI* site and a 3' *BamHI* site, and the PCR product was ligated into pIRESneo3, pIRESpuro3 and/or the pIRES2-DsRed bicistronic vector (Orthmann-Murphy et al., 2007) as previously described (Yum et al., 2007). The *GJB2* mutations were introduced into the ORF of human *GJB2* cDNA by PCR site-directed mutagenesis using the QuickChange kit (Stratagene, La Jolla, CA). To generate the mutations, mutagenic oligonucleotide primers were designed and incorporated using *Pfu-Turbo* DNA polymerase. The PCR products were digested by *Dpn*I endonuclease to eliminate the parental DNA template. The resulting DNA was used to transform XL-1 Blue bacteria, and minipreps were made from single colonies and sequenced at the Cell Center at the University of Pennsylvania. A large-scale plasmid preparation was made from a single colony (Qiagen) and the *GJB2* sequence with specific mutation was confirmed by direct sequencing. Human *GJB6* was obtained by RT-PCR (Superscript II; Invitrogen, Carlsband, CA) from human corpus callosum RNA (Clontech, Palo Alto, CA) and subcloned into the pIRESpuro3 vector as previously described (Yum et al., 2007).

Generating cell lines expressing Cx26, Cx30 or Cx26 mutants

Communication-incompetent HeLa cells (Elfgang et al., 1995) were obtained from Dr. Klaus Willecke, and grown in low-glucose Dulbecco's modified Eagle's Medium (DMEM) supplemented by 10% fetal bovine serum (FBS) and antibiotics (100 units/ml penicillin/100 μg/ml streptomycin) in a humidified atmosphere containing 5% CO_2 at 37°C. Transfection was carried out in 6 well plates as previously described (Yum et al., 2007). Briefly, Lipofectamine 2000 (Invitrogen, Carlsbad, CA) was incubated in Opti-MEM (GIBCO BRL, Carlsbad, California), and plasmids (containing wild type *GJB2*, individual human *GJB2* mutations or wild type *GJB6*, as well as plasmid alone) were incubated with Opti-MEM, both for 15 min at RT, then combined together for another 15 min. HeLa cells (approximately 80% confluent) were washed with Opti-MEM, incubated with the combined solution for 6 hrs at 37°C, washed with HBSS not containing calcium or magnesium, incubated for 2 days in DMEM at 37°, then selected by adding 1 μg/ml puromycin (Sigma-Aldrich, St. Louis, MO) or 1 mg/ml G418 (Invitrogen, Carlsbad, CA) to the medium over 3 weeks. The cells were trypsinized and these bulk-selected cells were expanded for further studies.

To generate stable cells expressing Cx30, the bulk-selected cells were plated at low density, and single colonies were picked and expanded. Cloned cells stably expressing Cx26 or Cx30 were obtaining by screening at least 30 different clones by immunostaining; of these, about 3–4 showed stable expression for at least 8 weeks. Control untransfected HeLa cells were also treated with puromycin or G418 and did not survive after about 10 days. To generate cells

expressing both Cx30 and Cx26 mutants, we chose one cloned cell line that stably expressed Cx30. This cell line was transfected with Cx26 in pIRESneo3 (or vector pIRESneo3 alone) according to the protocol described above. After selection with both 1 μg/ml of puromycin and 1mg/ml of G418 for about 3 weeks, the colonies were trypsinized and these bulk-selected cells were expanded for further studies. For transient transfection experiments, transfection was carried out using the Lipofectamine LTX reagent (Invitrogen, Carlsbad, CA) according to the manufacturer's "one tube" protocol, and the cells were analyzed ~40 hours after transfection.

Immunocytochemistry

HeLa cells were grown on coverslips for 2 days to ~70–90% confluency, washed in 1X PBS, fixed in acetone at −20°C for 10 min, blocked (5% fish skin gelatin in 1X PBS containing 0.1% Triton) for 1 hr in RT, and incubated overnight at 4°C with various antibodies diluted in blocking solution. As shown previously (Yum et al., 2007), a monoclonal antibody (Zymed Laboratories 33–5800, South San Francisco, CA; diluted 1:500) or a rabbit antiserum (Zymed Laboratories 51–2800, South San Francisco, CA, diluted 1:1000), both against the C-terminus of Cx26, and a rabbit antiserum against the C-terminus of Cx30 (Zymed Laboratories 71–2200, South San Francisco, CA; diluted 1:1000) did not cross-react with each other. We used these antibodies in our experiments, typically the combination of the mouse anti-Cx26 and the rabbit anti-Cx30. After washing in PBS, TRITC-conjugated donkey anti-rabbit, and FITC-conjugated donkey anti-mouse secondary antibodies were added in the same blocking solution (1:200) and incubated at RT for 1 hr. Coverslips were mounted with Vectashield (Vector Laboratories Inc., Burlingame, CA) and samples were photographed under a Leica fluorescence microscope with a Hamamatsu digital camera C4742-95 connected to a G5 Mac computer, using the Openlab 2.2 software for deconvolution.

Immunoblot analysis and co-immunoprecipitations

HeLa cells were grown to confluence on 100 mm plates, harvested in cold Dulbecco's PBS lacking Ca^{2+} and Mg^{2+} (Invitrogen, Carlsbad, CA). The supernatant was removed, the pellet was lysed in ice-cold lysis buffer (50 mM Tris, pH = 7.0, 1% dodesylsulfate (SDS), and 0.017 mg/ml phenylmethylsulfonyl fluoride (Sigma-Aldrich, St. Louis, MO), followed by a brief sonication (15 sec on, 10 sec off, for 6 times) on ice with a dismembrator (Fisher Scientific, Pittsburgh, PA). Protein concentration was determined using the BioRad Kit (Bio-Rad laboratories, Richmond, CA) according to manufacturer's instructions. For each sample, after 5–15 min incubation with electrophoresis buffer (62.5 mM Tris, pH = 6.8, 20% glycerol, 2% SDS, 100 mM DTT and bromophenol blue) at RT, 100 μg of protein lysates were loaded onto 12% SDS-polyacrylamide gel, electrophoresed and transferred to an Immobilon-polyvinylidene fluoride membrane (Millipore, Billerica, MA) using a semi-dry transfer unit (Bio-Rad, Hercules, CA), and blocked (5% blotting grade blocker non-fat dry milk and 0.5% Tween-20 in Tris-buffered saline) for 1 h. The blots were washed in blocking solution, incubated in peroxidase-coupled donkey antiserum against rabbit IgG (Jackson ImmunoResearch, West Grove, PA, diluted 1:10,000) for 1 h at RT. After washing in blocking solution and Tris-buffered saline containing 0.5% Tween-20, the blots were visualized by enhanced chemiluminescence (Amersham, Piscataway, NJ) according to the manufacturer's protocol.

For co-immunoprecipitations, HeLa cells grown to confluence on 60 mm plates were lysed in 500 μL of ice-cold RIPA buffer (10 mM sodium phosphate pH 7.0, 150 mM NaCl, 2 mM EDTA, 50 mM sodium fluoride, 1% NP-40, 1% sodium deoxycholate, and 0.1% SDS) for 15 minutes on ice, scraped, then spun at 14,000 rpm for 30 minutes. The supernatants were collected, and incubated on ice with 10 μl mouse monoclonal antibody against Cx26 for 1 hour. Protein G agarose (100 μl) was added to the above cell lysates/antibody solution, and incubated overnight at 4°C. The beads were washed in RIPA buffer, resuspended in electrophoresis buffer

(62.5 mM TRIS, 20% glycerol, 2% SDS, 100 mM DTT), separated on 12% SDS-polyacrylamide gel for protein detection following the immunoblotting protocol described. The blots were initially incubated with rabbit polyclonal antiserum against either Cx30 or Cx43, visualized, and then re-hybridized with a rabbit antiserum against Cx26.

Scrape-loading and fluorescence recovery after photobleaching (FRAP)

For scrape-loading, parental HeLa cells, bulk-selected cells that expressed wild type Cx26 (Cx26WT) or Cx26 mutants alone, or bulk-selected cells that co-expressed wild type Cx30 and Cx26 or one of the Cx26 mutants (or vector pIRESneo3 alone), were grown to confluence on 60 mm plates. The medium was changed to HBSS plus 0.1% Lucifer Yellow (LY; Sigma-Aldrich, St. Louis, MO), a fluorescent dye, or 2% neurobiotin (NB), a non-fluorescent tracer (Vector Laboratories, Burlingame, CA). Many parallel lines were cut into the dish with a razor blade, and after 5 min, cells scrape-loaded with LY were washed five times with HBSS, and imaged. Cells scrape-loaded with NB were fixed for 10 minutes in 4% paraformaldehyde at 4°C, blocked (5% fish skin gelatin in 1X PBS containing 0.1% Triton) for 1 hr in RT, and incubated with streptavidin-rhodamine diluted in blocking solution (1:300) for 1 hour at RT. After washing with PBS, coverslips were mounted with Vectashield (Vector Laboratories Inc., Burlingame, CA) and samples were photographed under a Leica fluorescence microscope with a Hamamatsu digital camera C4742-95 connected to a G5 Mac computer, using the Openlab 2.2 software. Scrape-loading was quantified by measuring the distance from the scrape line to the point where the average fluorescence intensity dropped to 1.5x the background intensity. For each cell line, this was measured for NB, by acquiring at least 8 images from each of three different plates of cells. The images were processed and analyzed with the NIH imageJ software and the mean distance was calculated using Microsoft Excel software, and compared between cell lines using ANOVA (GraphPad Prism 4 software, San Diego, CA).

For FRAP, bulk-selected cells co-expressing wild type Cx26 or one of the Cx26 mutants and Cx30 were grown on 35/22 mm glass bottom dish (Warner Instruments, Hamden, CT) for ~40 h to 70–90% confluency, washed in 1X HBSS, and incubated with calcein AM (1μM; Biotium, Haywood, CA) in Opti-MEM (Invitrogen, Carlsbad, CA) for 20 min, rinsed several times with 1X HBSS, and maintained in Opti-MEM at RT during the experiment. We used a 60x objective and the interactive software of a FluoView FV1000 Olympus laser scanning confocal microscope that has a synchronized laser scanning system, in which one laser provides high resolution image while the second laser stimulates simultaneously. Individual cells that were completely surrounded by other cells (at least 4 cells) were bleached by placing a cursor outlining the contour of the cells, and photobleached 7–8 times with a 405nm, 25mW diode laser at 90% power. The aim was to maximally bleach the selected cells, but not the neighboring cells. The 488-nm line of a 30-mW Argon laser at 0.3% excitation power of this instrument was used to detect the green fluorescence signal during the entire recording. To measure FRAP, images were acquired before bleaching and every 10 seconds following bleaching for 500 seconds. A circular cursor (slightly smaller than the cell) was placed in the center of the bleached cell, the average fluorescence intensity within the circle was measured as mean pixel density and exported (as an Excel file). One unbleached cell in the same field was also monitored for fluorescence loss throughout the experiment. In addition, individual cells that were isolated from the rest of the cells were also bleached and monitored for recovery in each dish; no recovery was observed (data not shown). Using Microsoft Excel software, the fluorescence signal intensity immediately prior and immediately after photobleaching was normalized to 100% and 0% respectively. Recovery was calculated based on the fluorescence intensity in the photobleached cell at each time point relative to the fluorescence intensity of the same cell at the same region prior to the bleaching and expressed as percent recovery.

FRAP was also performed and analyzed in HeLa cells transiently transfected with a pIRES2-DsRed bicistronic vector containing wild type *GJB2* or selected *GJB2* mutations using the protocol described above. The signal of DsRed was used as an indicator for transfected cells, and individual cells expressing DsRed surrounded by at least three other cells also expressing DsRed were chosen for bleaching and the recovery of fluorescence of the bleached cells were monitored for 400 seconds after bleaching.

To determine whether the FRAP of cells co-expressing Cx30 and individual Cx26 mutants differed from those of cells co-expressing Cx30 and Cx26 or Cx30 and the vector alone, we analyzed a model recovery curve of the FRAP results using a repeated measure nonlinear regression model with autocorrelated errors for the transformed percentages over time using Proc Mixed in SAS software (version 9.1). For each comparison of two cell groups, the nonlinear regression model consisted of linear and quadratic time effects, and group main and interaction effects with the linear and quadratic time factors. The test for difference between two group-specific mean curves (each curve is a specific cell line) was based on the test of significance of the two interaction parameters (the group-slope and the quadratic time interactions). The error terms were assumed to be autocorrelated to account for correlations among the responses across time within a given cell line. A p-value of < 0.05 was considered to be significant.

Supplementary Material

Refer to Web version on PubMed Central for supplementary material.

Acknowledgments

References

Ahmad S, et al. Connexins 26 and 30 are co-assembled to form gap junctions in the cochlea of mice. Biochem Biophys Res Commun 2003;307:362–368. [PubMed: 12859965]

Ahmad S, et al. Restoration of connexin26 protein level in the cochlea completely rescues hearing in a mouse model of human connexin30-linked deafness. Proc Natl Acad Sci U S A 2007;104:1337–41. [PubMed: 17227867]

Bakirtzis G, et al. Targeted epidermal expression of mutant Connexin 26(D66H) mimics true Vohwinkel syndrome and provides a model for the pathogenesis of dominant connexin disorders. Hum Mol Genet 2003;12:1737–1744. [PubMed: 12837696]

Beltramello M, et al. Permeability and gating properties of human connexins 26 and 30 expressed in HeLa cells. Biochem Biophys Res Commun 2003;305:1024–1033. [PubMed: 12767933]

Beltramello M, et al. Impaired permeability to Ins(1,4,5)P$_3$ in a mutant connexin underlies recessive hereditary deafness. Nat Cell Biol 2005;7:63–69. [PubMed: 15592461]

Brink PR, et al. Evidence for heteromeric gap junction channels formed from rat connexin43 and human connexin37. Amer J Physiol Cell Physiol 1997;42:C1386–C1396.

Bruzzone R, et al. Connections with connexins: the molecular basis of direct intercellular signaling. Eur J Biochem 1996;238:1–27. [PubMed: 8665925]

Bukauskas FF, et al. Gating properties of gap junction channels assembled from connexin43 and connexin43 fused with green fluorescent protein. Biophys J 2001;81:137–52. [PubMed: 11423402]

Chang Q, et al. Gap junction mediated intercellular metabolite transfer in the cochlea is compromised in connexin30 null mice. PLoS ONE 2008;3:e4088. [PubMed: 19116647]

Chen YY, et al. Mechanism of the defect in gap-junctional communication by expression of a connexin 26 mutant associated with dominant deafness. Faseb J 2005;19:U587–U602.

Cohen-Salmon M, et al. Targeted ablation of connexin26 in the inner ear epithelial gap junction network causes hearing impairment and cell death. Curr Biol 2002;12:1106–1111. [PubMed: 12121617]

Common JEA, et al. Cellular mechanisms of mutant connexins in skin disease and hearing loss. Cell Commun Adhesion 2003;10:347–351.

Common JEA, et al. Further evidence for heterozygote advantage of GJB2 deafness mutations: a link with cell survival. J Med Genet 2004;41:573–575. [PubMed: 15235031]

de Zwart-Storm EA, et al. A novel missense mutation in GJB2 disturbs gap junction protein transport and causes focal palmoplantar keratoderma with deafness. J Med Genet 2008;45:161–6. [PubMed: 17993581]

Di WL, et al. Connexin interaction patterns in keratinocytes revealed morphologically and by FRET analysis. J Cell Sci 2005;118:1505–1514. [PubMed: 15769851]

El-Fouly M, et al. Scrape-loading and dye transfer. A rapid and simple technique to study gap junctional intercellular communication. Exp Cell Res 1987;168:422–430. [PubMed: 2433137]

Elfgang C, et al. Specific permeability and selective formation of gap junction channels in connexin-transfected HeLa cells. J Cell Biol 1995;129:805–817. [PubMed: 7537274]

Estivill X, et al. Connexin-26 mutations in sporadic and inherited sensorineural deafness. Lancet 1998;351:394–398. [PubMed: 9482292]

Forge A, et al. Gap junctions in the inner ear: Comparison of distribution patterns in different vertebrates and assessment of connexin composition in mammals. J Comp Neurol 2003;467:207–229. [PubMed: 14595769]

Forge A, et al. Connexins and gap junctions in the inner ear. Audiol Neuro Otol 2002;7:141–145.

Gemel J, et al. Connexin43 and connexin26 form gap junctions, but not heteromeric channels in co-expressing cells. J Cell Sci 2004;117:2469–2480. [PubMed: 15128867]

Gerido DA, et al. Aberrant hemichannel properties of Cx26 mutations causing skin disease and deafness. Am J Physiol Cell Physiol 2007;293:C337–45. [PubMed: 17428836]

Grifa A, et al. Mutations in GJB6 cause nonsyndromic autosomal dominant deafness at DFNA3 locus. Nat Genet 1999;23:16–18. [PubMed: 10471490]

Haack B, et al. Deficient membrane integration of the novel p.N14D-GJB2 mutant associated with non-syndromic hearing impairment. Hum Mutat 2006;27:1158–9. [PubMed: 17041897]

Harris AL. Emerging issues of connexin channels: biophysics fills the gap. Q Rev Biophys 2001;34:325–472. [PubMed: 11838236]

Harris AL. Connexin channel permeability to cytoplasmic molecules. Prog Biophys Mol Biol 2007;94:120–43. [PubMed: 17470375]

Inoshita A, et al. Postnatal development of the organ of Corti in dominant-negative Gjb2 transgenic mice. Neuroscience 2008;156:1039–47. [PubMed: 18793701]

Jagger DJ, Forge A. Compartmentalized and signal-selective gap junctional coupling in the hearing cochlea. J Neurosci 2006;26:1260–8. [PubMed: 16436613]

Kelsell DP, et al. Connexin mutations in skin disease and hearing loss. Amer J Hum Genet 2001;68:559–568. [PubMed: 11179004]

Kelsell DP, et al. Connexin 26 mutations in hereditary non-syndromic sensorineural deafness. Nature 1997;387:80–83. [PubMed: 9139825]

Kikuchi T, et al. Gap junctions in the rat cochlea: immunohistochemical and ultrastructural analysis. Anat Embryol 1995;191:101–118. [PubMed: 7726389]

Kumar NM, Gilula NB. The gap junction communication channel. Cell 1996;84:381–389. [PubMed: 8608591]

Lautermann J, et al. Expression of the gap-junction connexins 26 and 30 in the rat cochlea. Cell Tissue Res 1998;294:415–420. [PubMed: 9799458]

Lee JR, et al. Connexin mutations causing skin disease and deafness increase hemichannel activity and cell death when expressed in Xenopus oocytes. J Invest Dermatol 2009;129:870–8. [PubMed: 18987669]

Liu YP, Zhao HB. Cellular characterization of Connexin26 and Connnexin30 expression in the cochlear lateral wall. Cell Tissue Res 2008;333:395–403. [PubMed: 18581144]

Maeda S, et al. Structure of the connexin 26 gap junction channel at 3.5 A resolution. Nature 2009;458:597–602. [PubMed: 19340074]

Manthey D, et al. Intracellular domains of mouse connexin26 and -30 affect diffusional and electrical properties of gap junction channels. J Membrane Biol 2001;181:137–148. [PubMed: 11420600]

Martin PEM, et al. Properties of connexin26 gap junctional proteins derived from mutations associated with non-syndromal hereditary deafness. Hum Mol Genet 1999;8:2369–2376. [PubMed: 10556284]

Marziano NK, et al. Mutations in the gene for connexin 26 (GJB2) that cause hearing loss have a dominant negative effect on connexin 30. Hum Mol Genet 2003;12:805–812. [PubMed: 12668604]

Matos TD, et al. A novel M163L mutation in connexin 26 causing cell death and associated with autosomal dominant hearing loss. Hear Res 2008;240:87–92. [PubMed: 18472371]

Michel V, et al. Molecular mechanism of a frequent genetic form of deafness. N Engl J Med 2003;349:716–7. [PubMed: 12917317]

Nagy JI, et al. Evidence for the co-localization of another connexin with connexin-43 at astrocytic gap junctions in rat brain. Neuroscience 1997;78:533–548. [PubMed: 9145808]

Orthmann-Murphy JL, et al. Two distinct heterotypic channels mediate gap junction coupling between astrocyte and oligodendrocyte connexins. J Neurosci 2007;27:13949–57. [PubMed: 18094232]

Oshima A, et al. Roles of Met-34, Cys-64, and Arg-75 in the assembly of human connexin 26 - Implication for key amino acid residues for channel formation and function. J Biol Chem 2003;278:1807–1816. [PubMed: 12384501]

Piazza V, et al. Functional analysis of R75Q mutation in the gene coding for Connexin 26 identified in a family with nonsyndromic hearing loss. Clin Genet 2005;68:161–166. [PubMed: 15996214]

Primignani P, et al. A novel dominant missense mutation - D179N - in the GJB2 gene (Connexin 26) associated with non-syndromic hearing loss. Clin Genet 2003;63:516–521. [PubMed: 12786758]

Richard G, et al. Missense mutations in GJB2 encoding connexin-26 cause the ectodermal dysplasia keratitis-ichthyosis-deafness syndrome. Amer J Hum Genet 2002;70:1341–1348. [PubMed: 11912510]

Stong BC, et al. A novel mechanism for connexin 26 mutation linked deafness: cell death caused by leaky gap junction hemichannels. Laryngoscope 2006;116:2205–10. [PubMed: 17146396]

Sullivan R, Lo CW. Expression of a connexin 43/beta-galactosidase fusion protein inhibits gap junctional communication in NIH3T3 cells. J Cell Biol 1995;130:419–29. [PubMed: 7542247]

Sun JJ, et al. Cochlear gap junctions coassembled from Cx26 and 30 show faster intercellular Ca^{2+} signaling than homomeric counterparts. Amer J Physiol Cell Physiol 2005;288:C613–C623. [PubMed: 15692151]

Sun Y, et al. Connexin30 null and conditional connexin26 null mice display distinct pattern and time course of cellular degeneration in the cochlea. J Comp Neurol 2009;516:569–79. [PubMed: 19673007]

Teubner B, et al. Connexin30 (Gjb6)-deficiency causes severe hearing impairment and lack of endocochlear potential. Hum Mol Genet 2003;12:13–21. [PubMed: 12490528]

Thomas T, et al. Functional domain mapping and selective trans-dominant effects exhibited by Cx26 disease-causing mutations. J Biol Chem 2004;279:19157–19168. [PubMed: 14978038]

Wang Y, et al. Targeted connexin26 ablation arrests postnatal development of the organ of Corti. Biochem Biophys Res Commun 2009;385:33–7. [PubMed: 19433060]

Wangemann P. K+ cycling and the endocochlear potential. Hear Res 2002;165:1–9. [PubMed: 12031509]

White TW, Bruzzone R. Multiple connexin proteins in single intercellular channels: connexin compatibility and functional consequences. J Bioenerg Biomembranes 1996;28:339–350.

Willecke K, et al. Structural and functional diversity of connexin genes in the mouse and human genome. Biol Chem 2002;383:725–737. [PubMed: 12108537]

Xia JH, et al. Mutations in the gene encoding gap junction protein −3 associated with autosomal dominant hearing impairment. Nat Genet 1998;20:370–373. [PubMed: 9843210]

Yum SW, et al. Human connexin26 and connexin30 form functional heteromeric and heterotypic channels. Am J Physiol Cell Physiol 2007;293:C1032–48. [PubMed: 17615163]

Zhang Y, et al. Gap junction-mediated intercellular biochemical coupling in cochlear supporting cells is required for normal cochlear functions. Proc Natl Acad Sci U S A 2005;102:15201–6. [PubMed: 16217030]

Zhao HB. Connexin26 is responsible for anionic molecule permeability in the cochlea for intercellular signalling and metabolic communications. Eur J Neurosci 2005;21:1859–1868. [PubMed: 15869481]

Zhao HB, Yu N. Distinct and gradient distributions of Connexin26 and Connexin30 in the cochlear sensory epithelium of guinea pigs. J Comp Neurol 2006;499:506–518. [PubMed: 16998915]
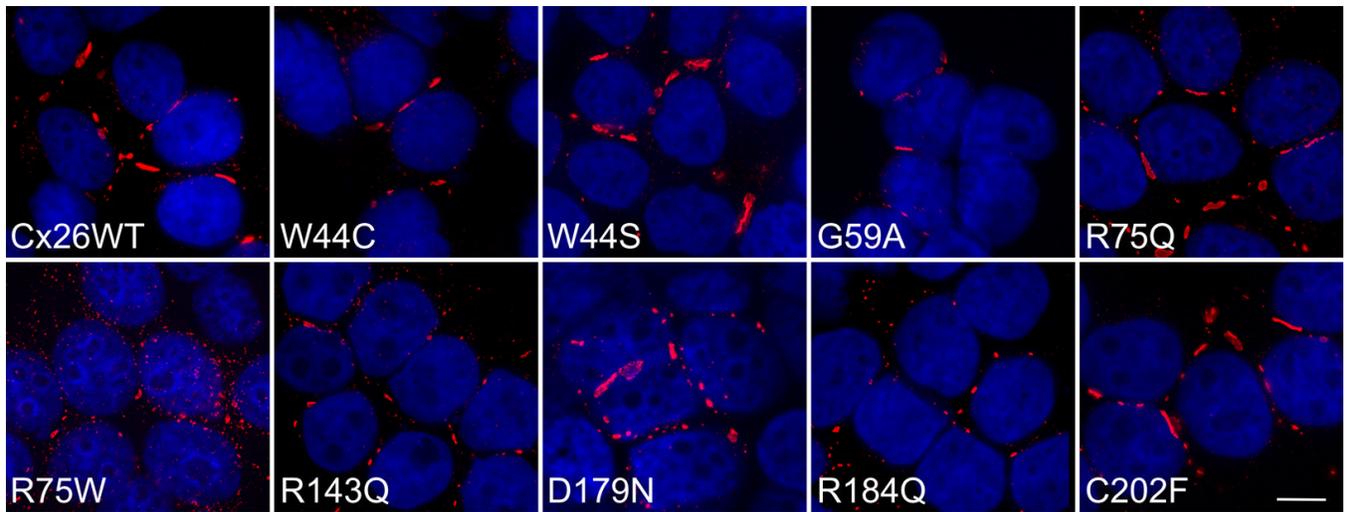
Figure 1. Dominant Cx26 mutants form gap junction plaques
These are deconvolved images of bulk-selected HeLa cells that express wild type human Cx26 (Cx26WT) or the indicated Cx26 mutant. The cells were labeled with a rabbit antiserum against the C-terminus of Cx26 (red) and counterstained with DAPI (blue). All cell lines had gap junction plaques at the cell borders; the R75W mutant had smaller plaques and more intracellular staining than the other mutants. Scale bar: 10 μm.
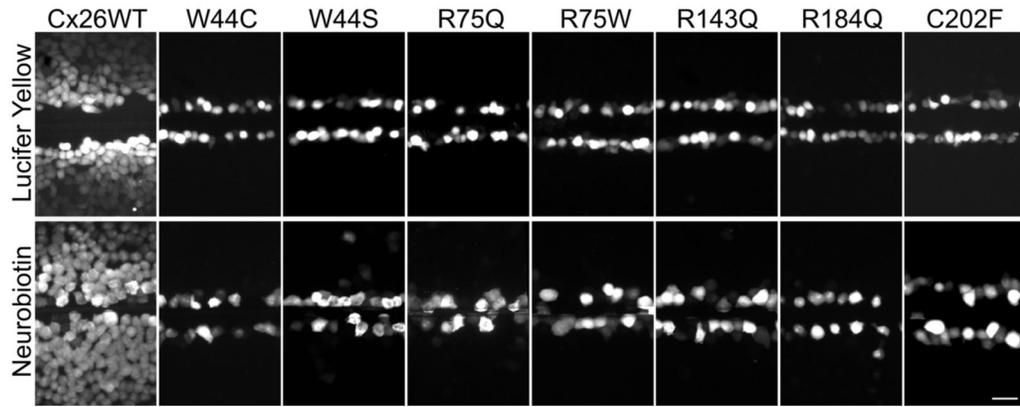
Figure 2. Dominant Cx26 mutants do not form functional gap junction channels
These are digital fluorescence images of confluent bulk-selected HeLa cells that stably express wild type Cx26 (Cx26WT) or the indicated Cx26 mutants. The cells were incubated in 0.1% Lucifer Yellow (LY, upper row) or 2% neurobiotin (NB, lower row), imaged (LY) or fixed (NB, then visualized with TRITC-conjugated avidin) ~15 min after being wounded with a scalpel blade. Note that the wounded cells picked up LY or NB in all cases, but only cells expressing Cx26WT showed extensive transfer of LY or NB to neighboring cells. Scale bar: 50 μm.
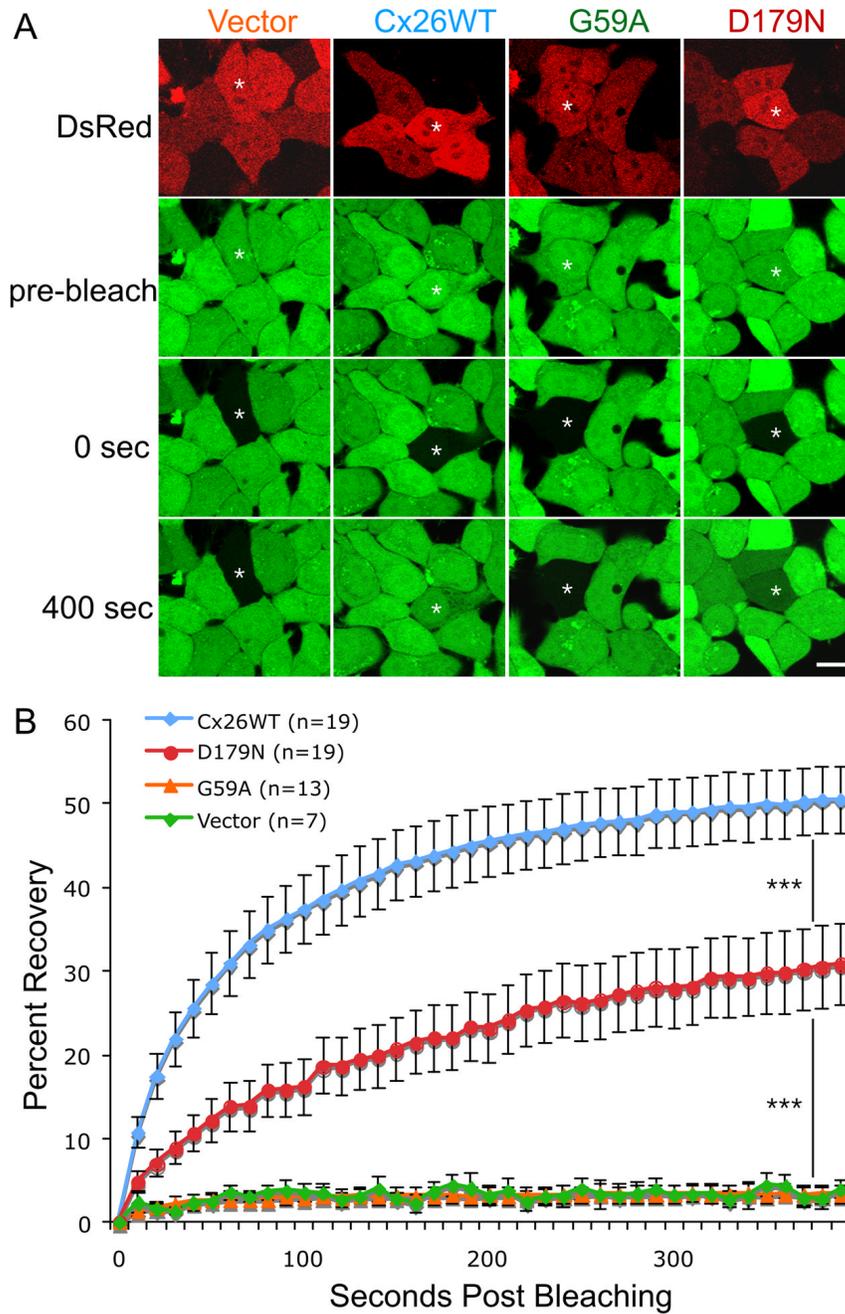
**Figure 3. The D179N mutant forms partially functional gap junction channels**
HeLa cells that were transiently transfected to express wild type Cx26 (Cx26WT), G59A, D179N, or the vector alone (vector). Two days later, the cells were incubated in calcein AM to fill the cytoplasm with calcein (green), and selected cells expressing DsRed (red) that were in close contact with at least three other DsRed-positive cells were photobleached, and then the green fluorescence signal was measured every 10 sec for 400 sec. Panel A shows examples of cells immediately before (pre-bleach), immediately after (0 sec), and 400 seconds after bleaching. Single asterisk (*) indicates the cells selected for bleaching. Scale bar: 10 μm. Panel B summarizes the FRAP data for many individual cells, by normalizing the fluorescent signal present in each cell immediately prior to and immediately after photobleaching to 100% and

0%, respectively. For each cell line, the curves connect the mean percent recovery at each time point from many individual cells as indicated; the vertical bars represent the means standard error. The recovery of the calcein signal in the bleached cells expressing D179N is more than that in cells expressing vector alone ($p < 0.0001$), but less than that in cells expressing Cx26WT ($p < 0.0001$). Triple asterisks (***) denotes a significance level of $p < 0.0001$.
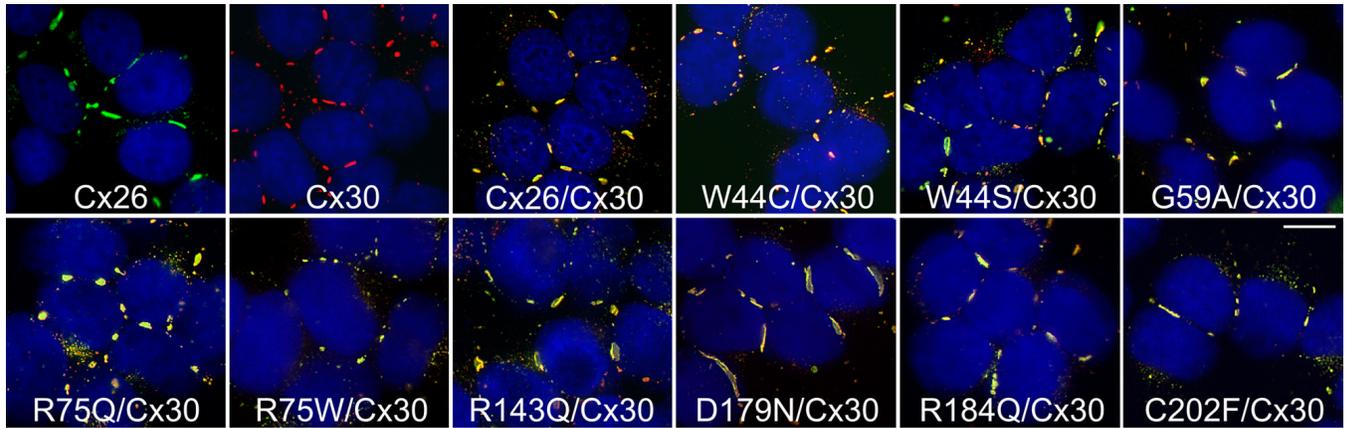
Figure 4. Cx26 mutants co-localize with Cx30
These are deconvolved images of bulk-selected HeLa cells that express wild type Cx26 or wild type Cx30 alone, or co-express wild type Cx30 and wild type Cx26 (Cx26/Cx30) or the indicated Cx26 mutant. The cells were double-labeled with a rabbit antiserum against the C-terminus of Cx30 (red) and a mouse monoclonal antibody against the C-terminus of Cx26 (green), and counterstained with DAPI (blue). In these merged images, Cx26 and Cx30 are largely co-localized, forming (orange to yellow) gap junction plaques at cell borders in all cases. Scale bar: 10 μm.
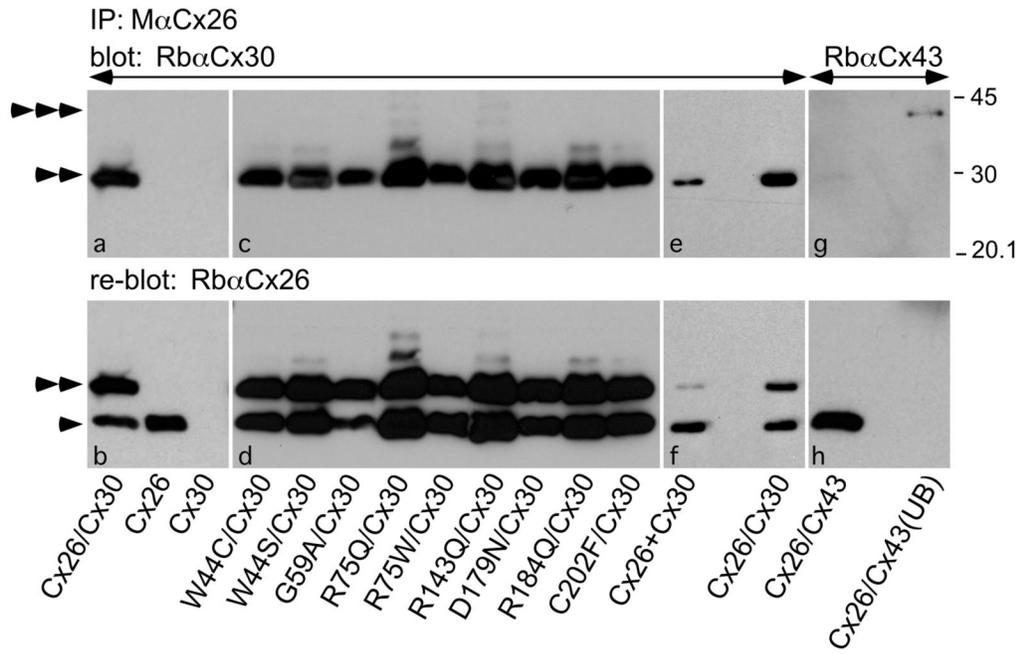
**Figure 5. Cx26 mutants co-immunoprecipitate Cx30**
Lysates were prepared from bulk-selected HeLa cells that stably express wild type Cx26, Cx30, or both Cx30 and Cx26 (Cx26/Cx30) or one of the Cx26 mutants as indicated (Cx26 mutation/Cx30), co-culture of stable Cx26 cells and Cx30 cells (Cx26+Cx30), as well as HeLa cells that were transiently transfected to express both Cx26 and Cx43 (Cx26/Cx43). The lysates were immunoprecipitated with a mouse monoclonal antibody against Cx26 (M Cx26), and the bound fractions or the unbound fraction were probed (upper panels) with a rabbit antiserum against Cx30 (Rb Cx30) or Cx43 (Rb Cx43), then reprobed (lower panels) with a rabbit antiserum against Cx26 (Rb Cx26). Note that M Cx26 co-immunoprecipitated Cx30 (double arrowhead), but not Cx43 (triple arrowheads), which is present in the unbound fraction (UB). Reprobing the blot reveals Cx26 in the appropriate samples (single arrowheads); the signal for Cx30 remains because the blot was not stripped before reprobing. Size markers (in kDa) are shown.
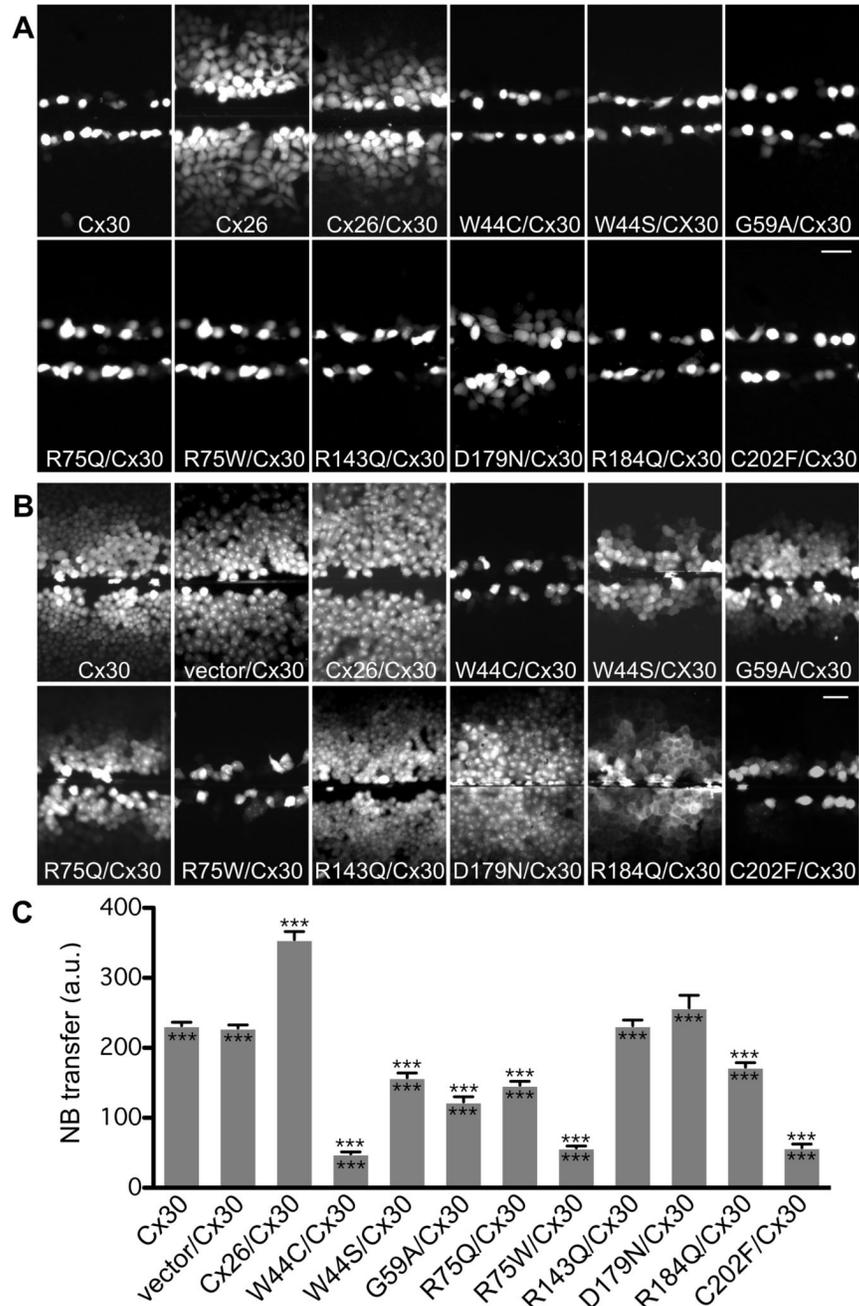
Figure 6. Dominant Cx26 mutants inhibit dye transfer of cells co-expressing Cx30
These are digital fluorescence images of confluent, bulk-selected HeLa cells that stably express wild type Cx30, or co-express Cx30 and an "empty vector" (vector/Cx30), as well as Cx26 (Cx30/Cx26) or the indicated Cx26 mutant. The cells were incubated in 0.1% LY (A) or 2% NB (B) for 5 min, and imaged either directly (LY) or following fixation (NB; visualized with TRITC-conjugated avidin) ~15 min after being wounded with a scalpel blade. In panel A, note that the wounded cells picked up LY in all cases, and, in contrast to cells expressing Cx30 alone, cells expressing Cx26 alone showed extensive transfer of LY to neighboring cells. None of the cells co-expressing a Cx26 mutant showed transfer of LY to neighboring cells except for cells co-expressing D179N, but this was less than in cells co-expressing wild type Cx26.

Scale bar: 50 μm. In panel B, note that NB transferred extensively in cells expressing Cx30 alone, or co-expressing Cx30 and wild type Cx26, R143Q, or D179N, less extensively in cells co-expressing Cx30 and W44S, G59A, R75Q or R184Q, and not at all in cells co-expressing Cx30 and W44C, R75W, or C202F. Scale bar: 50 μm. In panel C, quantitative analysis of intercellular NB transfer after scrape-loading is shown. The columns represent the mean distance of NB transfer from the scrape line to the point where the fluorescence intensity dropped to 1.5x the background intensity. For each cell line, this was measured by acquiring at least 8 images from each of two to three different plates of cells. The error bars indicate ± s.e.m. Triple asterisks (***) above the error bars denote a significance level of $p < 0.0001$ when compared to vector/Cx30 expressing cells, Triple asterisks (***) below the error bars denote a significance level of $p < 0.0001$ when compared to Cx26/Cx30 expressing cells.
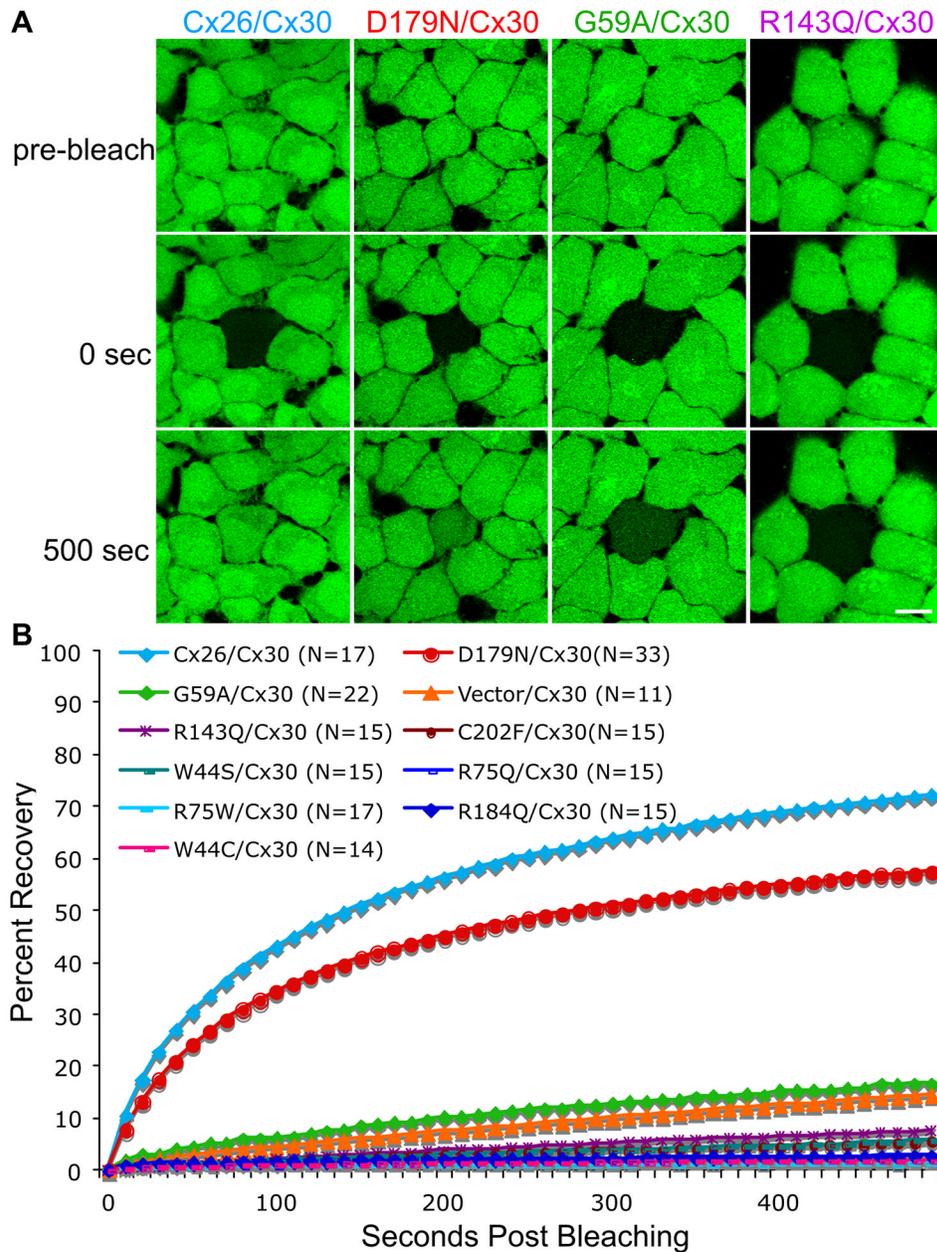
Figure 7. FRAP analysis of Cx26 and/or Cx30 gap junction channels
(A&B) Bulked-selected HeLa cells stably expressing wild type Cx30 or Cx26 alone, or co-expressing wild type Cx30 and Cx26 (Cx26/Cx30) or individual Cx26 mutants were incubated in calcein AM to fill the cytoplasm with calcein (green). Selected cells were photobleached, and the green fluorescence signal was measured every 10 sec for 500 sec. Panel A shows examples of cells immediately before (pre-bleach), immediately after (0 sec), and 500 seconds after bleaching. Scale bar: 10 µm. Panel B summarizes the data for many cells from individual cell lines, by normalizing the fluorescent signal present in each cell immediately prior to and immediately after photobleaching to 100% and 0%, respectively. The curves connect the mean percent recovery at each time point; standard errors are not shown. Note the robust recovery of the calcein signal in cells co-expressing Cx26/Cx30 or D179N/Cx30, but not in the bleached

cells co-expressing other Cx26 mutants or the vector alone. The statistical comparisons are shown in Table S1.